24th COBEM - 2017

24th ABCM International Congress of Mechanical Engineering
December 3-8, 2017, Curitiba, PR, Brazil

COBEM-2017-1543
A NUMERICAL STUDY ON THE EFFECT OF PLY ORIENTATION IN LAMB WAVE PROPAGATION THROUGH CARBON FIBER REINFORCED COMPOSITES

Luis Eduardo Jaramillo Bustamante
Humberto Brito Santana
Volnei Tita
Marcelo Leite Ribeiro
EESC/USP - University of São Paulo, São Carlos School of Engineering, Aeronatical Engeneering Department, Avenida João Dagnone, nº 1100, São Carlos, SP, Brazil
luis.jaramillo@usp.br
hbritosantana@gmail.com
voltita@sc.usp.br
malribei@usp.br

Abstract. *Lamb waves (LW) have been extensively proposed for long range inspection in composite structures oriented to Structural Health Monitoring (SHM). However, their propagation results complex to signal processing by their highly dispersive behavior. Better understanding of its propagation in composites is key to develop reliable damage detection strategies. LW propagation through a carbon fiber composite plate is simulated in Fem software Abaqus and its results are used to assess the effect of ply orientation on LW response. Stackings of* $[0]_8$, $[0/30]_{2S}$, $[0/60]_{2S}$ *and* $[0/90]_{2S}$ *excited with a Shear Vertical wave input at 50kHz were used. The propagation was sensed with equally spaced circular arrays of nodes; analogous to what would be an array of bonded piezo actuators/sensors of infinitely small radius. An analysis of numeric parameters setup was made. Signals comparisons and propagation speed distributions allowed to identify key features of the physical propagation phenomena despite of the simplifications made.*

Keywords: *lamb wave, wave propagation, composites, structural health monitoring, fem simulation*

1. INTRODUCTION

Composite materials offer a high stiffness-to-weight ratio when compared with metallic materials such as steel and aluminium. Their employ on aircraft has allowed the achievement of lighter structures which, in return, give a larger payload capacity per travel distance. Structures of recent aircrafts, such as the Boeing 787 Dreamliner and the Airbus A350-XWB, have been 45% made with composites (Staszweski *et al.*, 2008). However, their complex damage mechanics have been an obstacle that hinder a more extensive use and calls for a conservative Safe Life design approach (Tian *et al.*, 2015), or Damage Tolerance approach with higher inspection frequencies. Moreover, due to the possibility of damages hidden under the component's surface, such as low energy impacts, inspection becomes hard and expensive.

In this scenario, Structural Health Monitoring (SHM) have attracted a lot of attention since the last two decades. The basics of SHM consist in monitoring in real time critical and/or strategical zones of a structure aiming to collect a history of data that allows to determine its grade of degradation. Its key advantage lies in moving from a preventive maintenance philosophy to a condition-based maintenance philosophy (Balageas, 2006) in which the downtimes of an aircraft are defined not by scheduled inspections, but by exact maintenance tasks for a fully determined condition. Direct maintenance costs associated with inspections and reparations to the airframe structure were estimated by the International Aviation Transportation Association, IATA, from data reunited from 47 airlines worldwide in the order of 9 billion dollars in 2015; researchers such as Su *et al.* (2006) estimated a reduction of 30% in maintenance costs under an SHM scheme.

For this purpose, reliable Non-Destructive Tests (NDT) are mandatory, but they have to be also affordable. The main problem with traditional NDT, such as Ultrasonic Testing (UT) or visual inspection (VI), is that they become expensive once the structure size increases, a problem that worsens as the structure becomes old and inspection frequencies increase. To inspect an airplane's fuselage or wing using point-by-point UT have a great impact on direct operation costs for an operator. The latter has encouraged in the last decade the research in Acoustic Inspection (AI) with elastic waves on solids, or Lamb waves (LW). Lamb waves are defined as elastic waves propagating in an elastic solid with parallel free

boundaries and were described by the first time by Horace Lamb in 1917 (Su *et al.*, 2006). These waves offer the advantage of area-wide inspection capabilities, rather than point by point, like in UT, becoming attractive for large structures (Wan *et al.*, 2014).

Lamb waves are governed by the same wave equations as bulk waves, but exhibit an infinite number of vibration modes associated with their propagation (Staszweski *et al.*, 2008). For a given thickness *c* and frequency *f*, the number of propagating modes and wave velocities can be stablished from dispersion curves obtained from the Rayleigh-Lamb wave relations. However, for small values of the product *cf* there are mainly two modes propagating through the material: Symmetric fundamental, S_0, and Antisymmetric fundamental, A_0 (Staszweski *et al.*, 2008). In contrast to their practical advantages, this highly dispersiveness behaviour and composite's anisotropy impose hard to grasp technical challenges requiring to understand propagation when complexity-adding parameters, such as ply orientation in composite laminates, are manipulated so successful SHM strategies can be elaborated and evaluated. For the derivation of propagation equations, analytical methods range from 3D Elasticity (Brito *et al.*, 2015a) to asymptotical homogenization (Bensoussan *et al.*, 1978; Brito *et al.*, 2015b; 2015c). From the numerical point of view, works only focus in simulating damage detection for a fixed composite stacking (Samaratunga and Jha, 2012; Wang *et al.*, 2012) obtaining, at first, only particular results.

The main objective of the present work is to numerically demonstrate the isolated effect of introducing different grades of anisotropy on Lamb wave propagation on composites and to study how it would affect considerations for damage detection strategies on composite parts. Also, a comprehensive explanation of simulation parameters setting is presented with the intention of this work to become an introduction and practical guide to simulation of elastic waves.

2. METHODOLOGY

2.1 Computational domain and strategy

For this study, a CFRP composite plate is modelled in Abaqus. Plate dimensions are 300 mm width by 450 mm long, as shown in Fig. 1. The X_1 direction is aligned with the longest side, and the fibre-orientation is measured with respect to it. This domain is partitioned in three circles of radius 25 mm, 50 mm, and 75 mm, referred as 1st, 2nd and 3rd circle respectively. All circles are coincident with the excitation's origin as shown in Fig.1. At the same time, every quarter of a circle is divided into three equal areas and sensor nodes are defined in each intersection between circles and linear divisions, as highlighted for the 30° direction. The notation used to identify the sensor nodes employs the counter clockwise angle of the segment line with respect to X_1 and then is followed by the specific circle's number, for instance: N30-2 means the node in the intersection of the 2nd circle (50 mm from the centre) with the line segment at 30° from X_1. Fixed boundary conditions in the right and left sides are also defined as shown in Fig. 1.

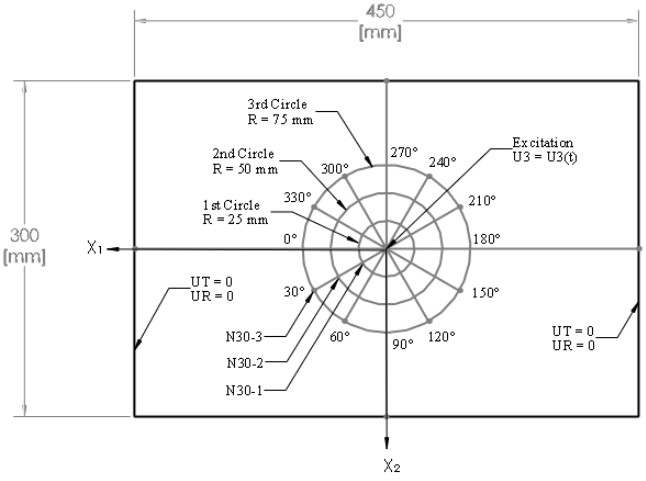

Figure 1: CFRP plate model's domain, partitions, and boundary conditions.

The numerical strategy consists in that, once the burst is applied, the wave propagates and the out of plane displacement, U3, and the signal arrival times are measured in the sensor nodes. It is important to notice that, for a same partition circle, the fibre orientation with respect each nodal position vector varies, allowing to see its effect on the response when nodes in the same circle are analysed. In the same way, for a same segment line, the distance between each node and the centre varies, allowing to see its effect on the response when nodes in the same line are analysed. Also, the signal arrival times allow to plot the in-plane distribution of the phase velocity, so patterns can be observed. This procedure is first done on an 8-ply unidirectional CFRP plate, this is a $[0]_8$ configuration. Then, the procedure is repeated

for 8-ply plate in $[0/30]_{2S}$, $[0/60]_{2S}$, and $[0/90]_{2S}$ configurations. This is used to assess the effect on propagation of introducing different grades of anisotropy, starting with the most anisotropic configuration, and varying fibre orientation until the most isotropic, as shown in Fig. 2 using the stiffness ratio for in-plane directions (calculated using the classical lamination theory homogenization).

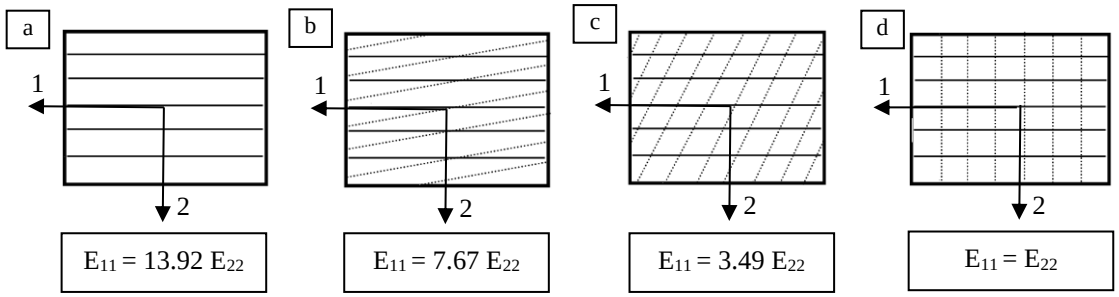

Figure 2: Stiffness ratio of in-plane directions for various 8-ply configurations; (a) $[0]_8$, (b) $[0/30]_{2S}$, (c) $[0/60]_{2S}$, (d) $[0/90]_{2S}$.

2.2 Material Modelling

The plate is modelled with 8 plies of 0.288 mm thick CFRP prepregs for a total thickness of 2.304 mm. Orthotropy is assumed with plane 2-3 as plane of isotropy. Mechanical properties for the used material are shown in Tab. 1.

Table 1: CFRP material properties employed.

Property	Value
E_{11}	127 GPa
$E_{22} = E_{33}$	10 GPa
$\upsilon_{12} = \upsilon_{13}$	0.34
υ_{23}	0.306
$G_{12} = G_{13}$	5.44 GPa
G_{23}	3.05 GPa
ρ	1580 kg/m3

2.3 Actuation modelling

The actuation modelling is heavily associated with the means of excitation. For SHM the most common and practical mean of excitation have been the use of piezoelectric actuators. When an oscillating voltage difference is applied, these actuators strain, and so they transmit strains on the specimen's contact surface area that propagates through the material. The coupling of the mechanical and electric effects on the piezoelectric actuators add complexity to the wave propagation behaviour; so, to isolate the effect of the fibre-orientation on propagation, the actuation was modelled as nodal oscillatory displacement profile in the X_3 direction that propagates in the X_1-X_2 plane, this is, shear vertical (SV) waves were generated on the specimen by an out-of-plane displacement input generated by a piezo actuator of infinitesimal diameter.

The input excitation profile has another set of considerations. Initially, the variables involved are excitation frequency, propagation mode, shape, number of cycles and signal amplitude (Jaramillo and Ribeiro, 2017). Excitation frequency selection must be such that the less possible dispersive behaviour is achieved, this is, it is desired to have the less quantity of vibration modes existing on the specimen so a response easier to read and interpret is obtained (Staszweski et al., 2008). The latter is especially important for damage detection schemes. For a CFRP specimen, for instance, a frequency-thickness product of less than 1 MHz·mm is considered good due to the existence of only the fundamental symmetric and the antisymmetric modes, S_0 and A_0 respectively (Monnier et al. 2006). In the other hand, the number of cycles affects the dispersiveness; the larger the number of cycles, the narrower the bandwidth and less dispersiveness is obtained. However, a large number of cycles also contributes to complex reflection patters and noisy responses that could become troublesome to interpret (Staszweski et al., 2008).

Considering the above statements, the function defining the excitation's displacement to be used is a modulated Hann Window given by Eq. (1).

$$U_3(t) = \begin{cases} \frac{-A}{2}\sin(2\pi f t)\left(1-\cos\left(\frac{2\pi f t}{N}\right)\right) & t \le T = N/f \\ 0 & t > T = N/f \end{cases} \quad (1)$$

Where $U_3(t)$ is the displacement instantaneous magnitude. *A* is the burst amplitude, *f* is the central frequency, *N* is the number of cycles and *T* is the total excitation time. The values of these parameters are chosen as the same used in the studies of Samaratunga (2012) and Wang et al. (2012), which were chosen to minimize dispersiveness. Such parameters are condensed in Tab. 2 and the entire function is plotted in Fig. 3.

Table 2: Input excitation's parameters values.

Property	Value
A	1 µm
f	50 kHz
N	3.5
T	70 µs

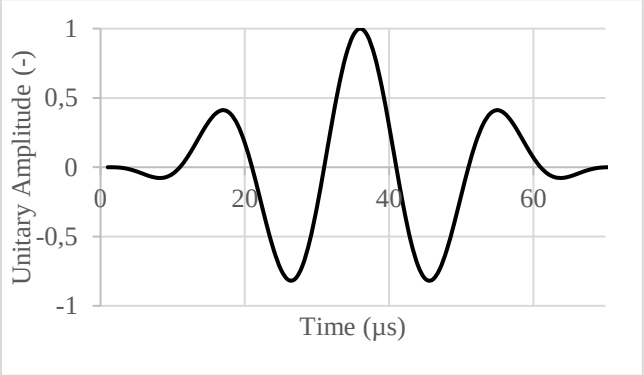

Figure 3: Excitation tone burst profile, in m vs. µs.

2.4 Numerical parameters set-up

The propagation study was done through a Dynamic analysis in Fem software Abaqus. The analysis method chosen was Implicit Integration because is easier to achieve numerical stability and accuracy with it. This method has the backdown of increased computation time but, due to the problem being small in domain size, the computation cost penalty associated with it is not high. The element size must be selected such there are in between 10 and 20 elements per wavelength (Wang *et al.*, 2012), so it becomes easier to capture the wave response. To determine the theoretical wavelength, the theoretical phase velocity must be used. Phase velocity for anisotropic materials can be obtained solving the Christoffel equation (Tsvankin, 1997):

$$\left[C_{ijkl}n_j n_l - \rho V^2 \delta_{ik}\right]U_k = 0 \tag{2}$$

Where C_{ijkl} is the material's (i.e. laminate's) stiffness tensor, *n* is the unit vector in the propagation direction, *V* is phase velocity, δ_{ij} is the Kronecker's delta and U_k is the displacement vector. Then, solving the eigenvalue problem of eq. 2, the shear vertical wave phase velocities in directions 1 and 2 are:

$$V_1 = \sqrt{\frac{C_{1212}}{\rho}} \tag{3}$$

$$V_2 = \sqrt{\frac{C_{2323}}{\rho}} \tag{4}$$

The C_{1212} and C_{2323} components from the laminate stiffness tensor were obtained by asymptotic homogenization (Bensoussan *et al.*, 1978). These velocities vary with the mechanical properties of each laminate considered. In this case, the fastest phase velocities are expected in the unidirectional configuration, $[0]_8$, so the mechanical properties of this laminate are used. In whichever case, the wavelength, λ_i, is:

$$\lambda_i = \frac{V_i}{f} \tag{5}$$

With this information, the element size, *h*, can be estimated. This calculation gives an estimate and 1.389 mm of element size and a size of 1mm is selected for more precision. This value also is coherent with the ones used in works such as done by Samaratunga and Jha (2012), and Wang *et al.* (2012) of 2 mm and 1 mm, respectively. Meshing with this element size resulted in 148269 linear four node shell elements with reduced integration, S4R in Abaqus syntax. Also, the total number of nodes were 149020.

Also, time step used was of 1μs and a total time of 200 μs was chosen so the analysis finishes when the wave had propagated completely through the sensor nodes (reflections and related features are not of interest for this work), thus saving computation time. All this information is resumed in Tab. 3.

Table 3: Dynamic analysis meshing and time parameters.

Direction	*V*	λ	*h*	Element Type	Number of Elements	Number of Nodes	Time Step/ Total Time
1	1855 m/s	37.1 mm	1.855 mm	S4R	148269	149020	1 μs
2	1389 m/s	27.8 mm	1.389 mm	-	-	-	200 μs

3. RESULTS AND DISCUSSIONS

The out-of-plane displacement response in every sensor was measured and normalized with respect to their correspondent maximum value for comparison purposes. However, as shown in an example response in Fig. 4, the actual response shows an amplitude decay due to the spreading of the energy per unit area through the plane; or more specifically, energy conservation. This decay should not be attributed to material damping, which was not specified; however, the decay has some degree of numerical damping attributed to the implicit integrator used, which, by Abaqus default, is set as Hilbert-Hughes-Taylor (HHT) integrator (Simulia, 2015).

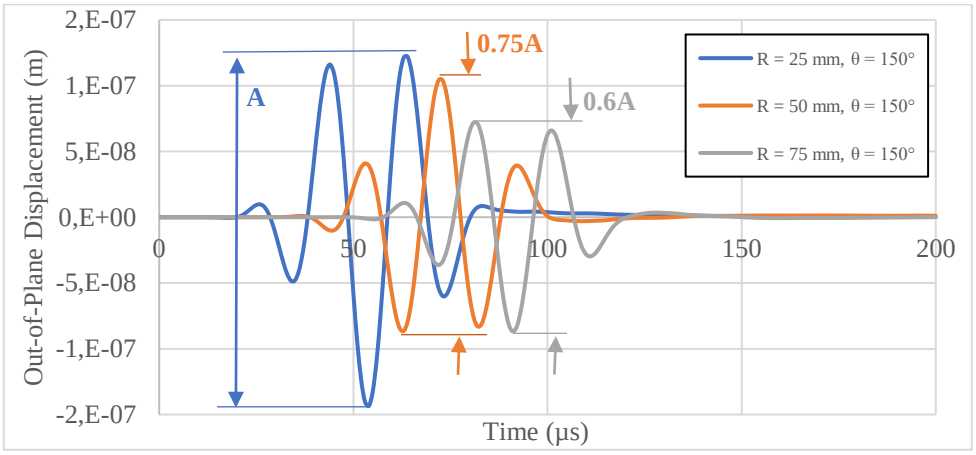

Figure 4: Out-of-Plane displacements for the [0]8 configuration, along de θ = 150° direction.

The mean amplitude decay was found to be very similar in all plate configurations, hence unaffected by fibre orientation at first glance. At 50 mm, the mean decay was about a 25% (+/- 3%) of the amplitude measured at 25mm. At 75 mm, the amplitude had decayed about a 40% (+/- 3%) of the amplitude measured at 25 mm. It must be noticed that these values are only valid for free propagation through the plane and, in general, the amplitude decay is a parameter that should be accounted in the designing of a damage detection strategy in composites. The latter will be an input for the optimization of sensor location in a given structure, since it may define the sensitiveness of the SHM system and, with it, its practical range of inspection.

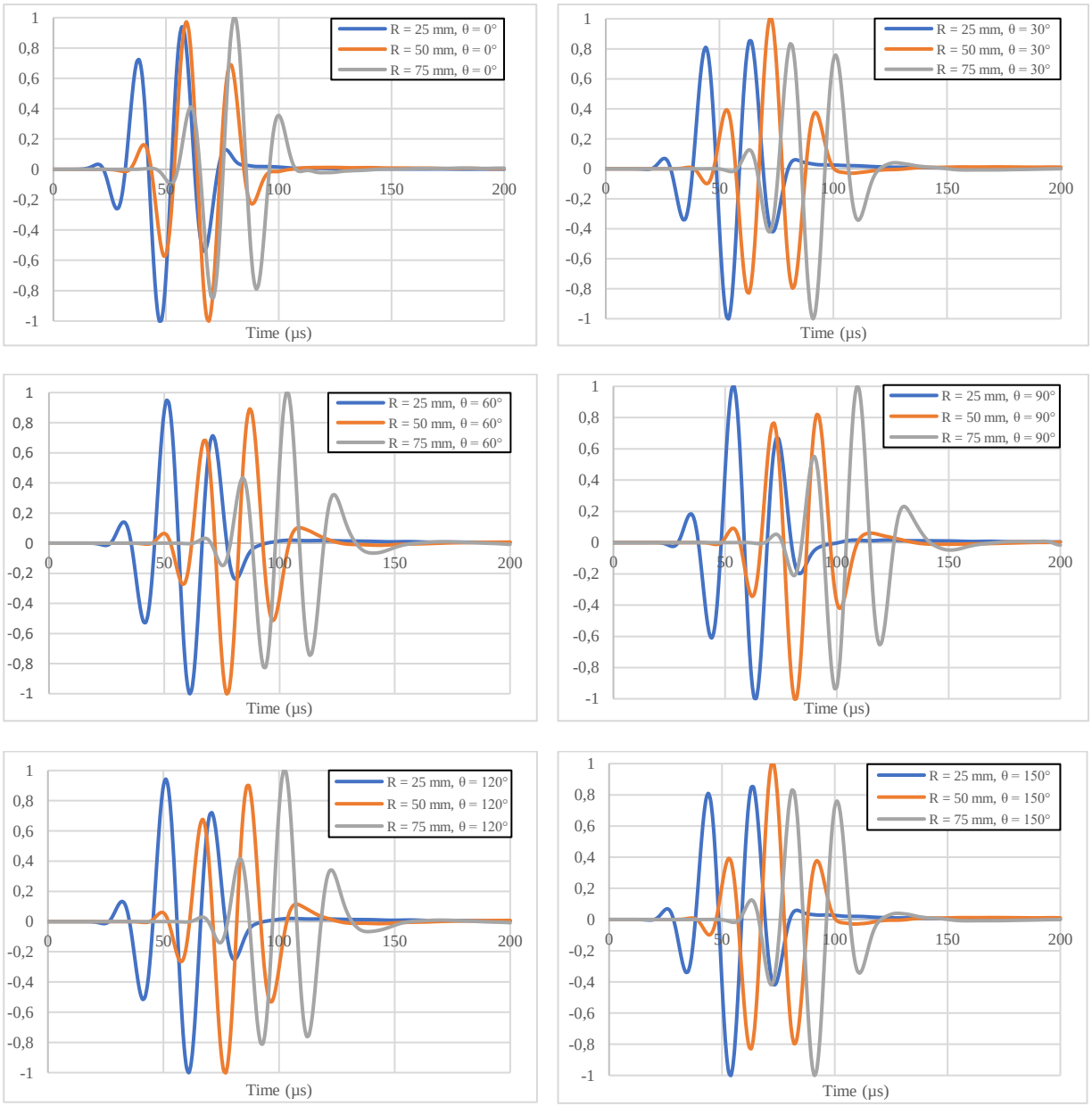

Figure 5: Normalized out-of-plane displacements for the $[0]_8$ configuration for the (a) 0°, (b) 30°, (c) 60°, (d) 90° direction.

Figure 5 shows the responses in node sensors along the various radii and sweeping half a circumference of propagation for the $[0]_8$, this is, the most anisotropic case. It should be noticed that, for this configuration, the response is symmetrical along $\theta = 0°$ and 90°, i.e. the response at $\theta = 30°$ is the same as 330° and 150°, due to the aligned fibres. One of the most important aspect of the responses is their shape. It changes when propagating through fixed and variable radius, showing other practical complexity for signal interpretation: quasi-continuous mode conversion. As explained, at low frequencies coexist the symmetric and antisymmetric vibration modes, the phenomenon, as described by Hennings and Lammering (2016), appears after the fastest guided wave (i.e. S_0 in isotropic solids) has passed the observed area and before de second fastest wave (i.e. A_0 in isotropic solids) arrives. In this period, regular patterns occur which are not seen in isotropic solids. This phenomenon can be of use for detecting damage in composites, but its study is still recent (Hennings and Lammering, 2016). The $[0/30]_{2S}$, $[0/60]_{2S}$ and $[0/90]_{2S}$ present the same mode conversion phenomenon as shown for various response samples shown in Fig. 6.

Other effect of the different grades of anisotropy introduced by fibre orientation, is the values and profiles of the in-plane shear wave phase velocity distribution. Figure 7 shows how fibre orientation gives a “shape” to propagation, starting from an elliptic shape in the most anisotropic case, up to approximately a circle in the most isotropic case. In a damage detection scheme, this is useful for strategies dependant on the signal’s time of flight so accurate comparisons between pristine and damaged configurations can be done.

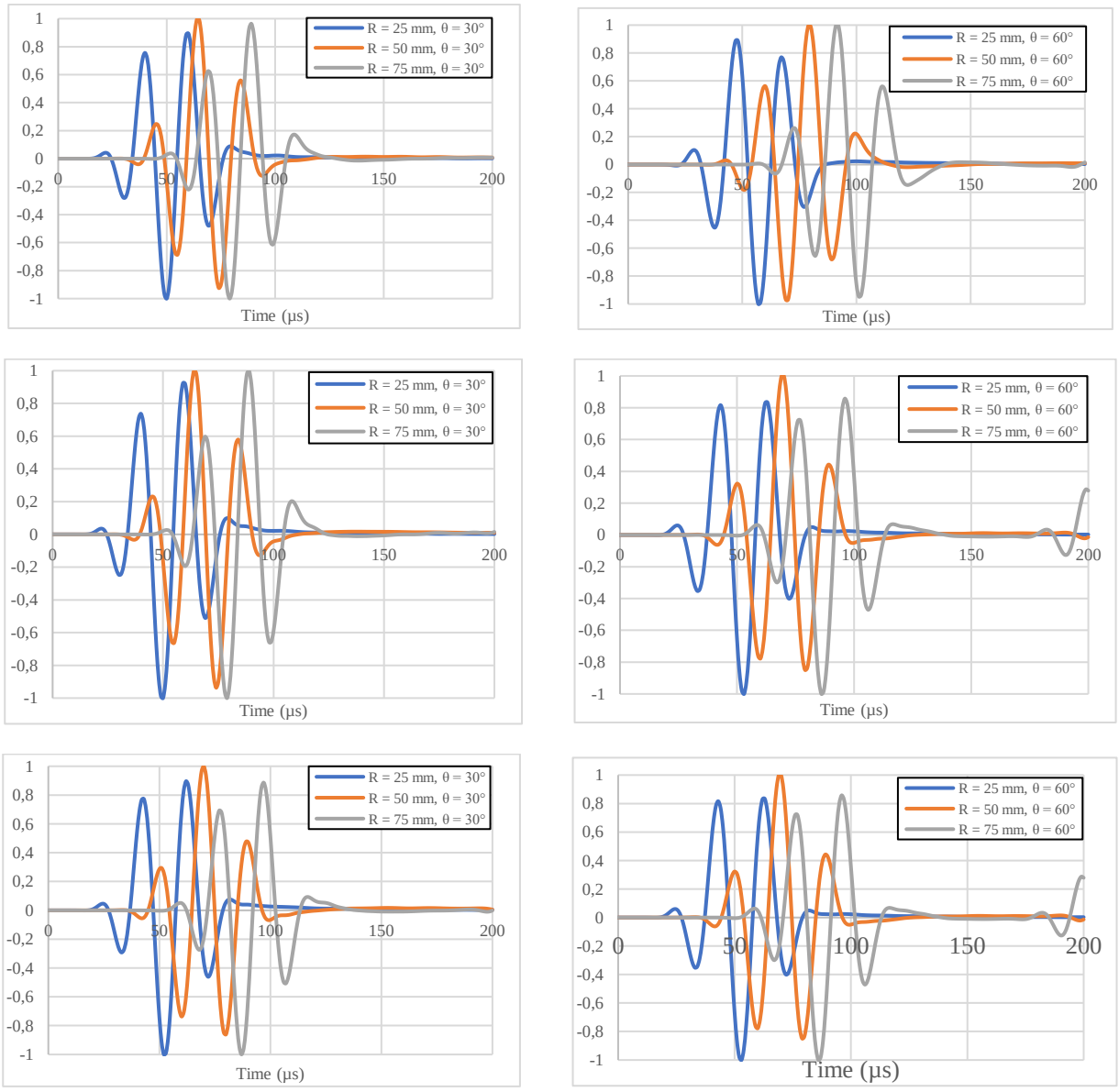

Figure 6: Normalized out-of-plane displacement samples for (a) $[0/30]_{2S}$, (b) $[0/60]_{2S}$ and (c) $[0/90]_{2S}$ laminates in the 30° and 60° directions.

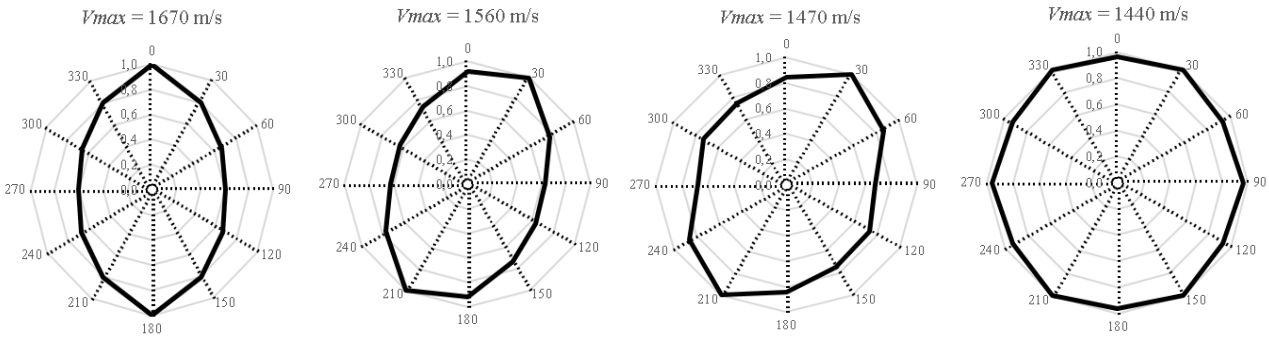

Figure 7: In-plane phase velocity distribution normalized to the maximum mean velocity *Vmax*.

Conclusions

The fiber orientation effect on the propagation of Lamb waves, in the form of shear vertical waves, in composite media through numerical means for various stacking configurations was studied and its implications on damage detection strategies development was discussed. It was observed how the adding of anisotropy in the different stackings ended in a mode conversion effect on the response wave, which adds both opportunities and complexities to the task of damage detection on composites. Also, the main purpose of this work was to be used as a guide into dynamic simulation of lamb waves.

Future work based on this results include the modelling of piezo actuators and sensors and running the same test to compare the effect of piezo diameter on the response, which would allow to assess the possibility of dimension optimization. Also, the introduction damages typical to composites such as delamination would allow to assess their effect on propagation in order to identify opportunities within the input excitation parameters tunning.

The results of the present work are also going to be used to assess analytical models involving asymptotical homogenization, that is in ongoing work by the authors.

4. REFERENCES

Bensoussan, A., Lions, J.L., Papanicolaou, G., 1978. *Asymptotic analysis for periodic structures*. North-Holland, New York.

Brito-Santana, H., Wang, Y., Rodríguez-Ramos, R., Bravo-Castillero, J. and Guinovart-Díaz, R., 2015a. "A dispersive nonlocal model for shear-wave propagation in laminated composites with periodic structures". *European Journal of Mechanics and Solids*, Vol. 49, p. 35–48.

Brito-Santana, H., Wang, Y., Rodríguez-Ramos, R., Bravo-Castillero, J. and Guinovart-Díaz, R., 2015b. "Dispersive shear-wave propagation in a periodic layered composite with imperfect interfaces", *International Journal of Automotive Composites*, Vol. 1, p. 184–204.

Brito-Santana, H., Wang, Y., Rodríguez-Ramos, R., Bravo-Castillero, J., Guinovart-Díaz, R. and Tita, V., 2015c. "A dispersive nonlocal model for in-plane wave propagation in laminated composite with periodic structures". *Journal of Applied Mechanics*, Vol. 82, p. 031006-1–031006-15.

Giurgiutiu, V., 2005. „Tuned lamb wave excitation and detection with piezoelectric wafer active sensors for structural health monitoring". *Journal of Intelligent Materials Systems and Structures*, Vol. 16, p. 291–305.

Hennings, B., Lammering, R., 2016. "Material modeling for the simulation of quasi-continuous mode conversion during Lamb wave propagation in CFRP-layers". *Composite Structures*, Vol. 151, p. 142-148.

Samaratunga, D. and Jha, R., 2012. "Lamb wave propagation simulation in smart composite structures". In *Simulia Community Conference Proceedings*. Rhode Island, United States.

Tian, Z., Yu, L. and Leckey, C., 2015. *Guided wave propagation study on laminated composite by frequency-wavenumber technique*. Report, NASA Langley Research Center.

Wan, X., Zhang, Q., Xu, G., and Tse, P.W., 2014. "Numerical simulation of nonlinear lamb waves used in a thin plate for detecting buried micro-cracks". *Sensors*, Vol. 14, p. 8528–8545.

Wang, J.T., Ross, R.W., Huang, G.L. and Yuan, F.G., 2013. *Simulation of detecting damage in composite stiffened panel using lamb waves.* Report, NASA Langley Research Center.

Wilberg, C., Duczek, S., Vivar Perez, J. M. And Ahmad, Z. A. B., 2015. „Simulation methods for Guided wave-based Structural Health Monitoring: A review". *Applied Mechanics Reviews*, Vol. 67, p. 010803-1–010803-20.

Yang, C., Ye, L. and Bannister, M., 2006. "Some aspect of numerical simulation for lamb wave propagation in composite laminates".

5. RESPONSIBILITY NOTICE

The authors are the only responsible for the information included in this paper.

6. ACKNOWLEDGEMENTS

The authors acknowledge the valuable financial support of *CAPES, CNPq* and *FAPESP (2015/13844-8)* which made this work possible. Also, the valuable technical and scientific support of the *Aeronautical Structures Group* of the São Carlos School of Engineering at the University of São Paulo.